CENTRE FOR
SYSTEMS
SCIENCE

LCCR

Simon Fraser University, Burnaby, B.C., Canada V5A 1S6 / (604) 291-4704

The Performance of Phase Locked TTIB with Symmetric Phase Detection

James K. Cavers

CSS/LCCR TR 89-06

92-05563/

THE PERFORMANCE OF PHASE LOCKED TTIB WITH SYMMETRIC PHASE DETECTION

by

James K. Cavers

School of Engineering Science
Simon Fraser University
Burnaby B.C. V7E 1Z8
CANADA

Tel. (604) 291-3281

June 1989

ABSTRACT

Transparent tone-in-band (TTIB) creates a spectral gap by splitting a signal into frequency bands, which are then separated by modulation. The receiver recombines the bands by demodulation, a process which must be coherent in the case of data transmission. Phase locked transparent-tone-in-band (PLTTIB), in its original form, contained an unacceptably high level of self-noise in the coherent band recombination process. Recently, a symmetric form of the PLTTIB phase detector has been demonstrated to eliminate self-noise, though no analysis of its locking behaviour has been available. This paper provides the first performance analysis of PLTTIB with symmetric phase detection, and contains a number of results of importance to the designer, including the effect of recombination phase error on BER, the mean square phase error, the pdf of phase error, and the pull-in time of the phase tracker. Although the detailed results are obtained only for static channels, a qualitative assessment of the effect of fading is given.

This work was supported by the British Columbia Advanced Systems Institute.

I INTRODUCTION

A number of recent papers [1-5] have analyzed the use of a pilot tone to assist the transmission of data through rapidly fading channels. Among the advantages are the suppression or elimination of the irreducible error rate which is characteristic of these channels, and the ability to employ multilevel modulation formats, and thereby gain higher data rates in the limited bandwidth available. Much of the current work in pilot tone assisted transmission has centered on two problems with the method: the question of where to put the tone, and the fact that the envelope is not constant.

Transparent tone-in-band (TTIB) [1,2,5] is an unusual solution to the first problem. The transmission band is split into separate subbands, which are moved apart by modulation to create a gap into which the pilot tone can be placed. The receiver reverses the process, recombining the subbands into what should be a replica of the original signal. TTIB is not tied to a particular modulation technique; it works for any signal, analog or digital, and the gap can be made as wide as desired. Moreover, its use is not limited to pilot tone systems; the gap can be used for carrying in-band signals such as "scribblephone" data, or for circumventing the loss of low frequencies in AC coupling.

However, when TTIB is used to carry data signals, the receiver oscillator used for recombining the frequency bands must be phase locked to that in the transmitter, or the signal is distorted and an unacceptable bit error rate results. Phase locked TTIB (PLTTIB) [3] was proposed as a way of achieving lock without requiring transmission of an explicit synchronization signal, such as another tone. However, the method has been shown [6] to generate a high level of self noise, resulting in very long acquisition times.

A recent paper by Bateman [7] has demonstrated that a symmetric form of the PLTTIB phase detector can eliminate the self noise, although no performance analysis was given.

The present paper provides the missing analysis of symmetric PLTTIB, and contains three principal contributions. It presents a phase detector which is simpler than that in [7], and offers slightly better performance. It evaluates the effect of recombination phase error on BER performance. Finally, it analyses the locking behaviour and the

recombination phase error variance of symmetric PLTTIB, including the time for initial pull-in. The results are of principal interest for data, but the phase jitter analysis is also valid for voice or other analog signals.

II TTIB PROCESSING

Overall Structure

Figure 1 illustrates the overall structure of a TTIB system. The incoming information signal v(t) can represent a general complex QAM data signal. Alternatively, it can represent the upper or lower sideband of a voice signal, shifted to a 0 Hz center, as in the Weaver method of generating SSB signals. TTIB band separation, described below, creates a spectral gap in which a pilot tone is inserted. The channel introduces random amplitude and phase fluctions and adds white Gaussian noise. At the receiver, the pilot tone provides the basis for AGC and phase correction [1,3,4] After removal of the tone, the receiver recombines the separated bands, to create a reproduction of the transmitted signal v(t). In this paper, we focus on the band recombination process, since the mechanics of pilot tone processing are well known.

Transmitter Processing

Figure 2 illustrates TTIB's band separation processing, with heavy lines used to indicate complex baseband signals. A pair of complex bandpass filters $H_{l+}(f)$ and $H_{l-}(f)$ select the positive and negative bands, respectively, of the input signal v(t). A gap centered at 0 Hz is formed by shifting the bands by multiplication with complex carriers $\exp(\pm j2\pi f_s t)$. A pilot tone can then be inserted into the gap simply by adding a dc level. The analysis below ignores the pilot, though, since our interest is in band recombination, rather than pilot tone processing. The transmitted complex envelope z(t) is therefore represented in the frequency domain by:

$$Z(f) = V(f-f_s)H_{l+}(f-f_s) + V(f+f_s)H_{l-}(f+f_s) \qquad (1)$$

TTIB increases the bandwidth by $2f_s$, as illustrated in Figure 3.

The bandpass filters $H_{l+}(f)$ and $H_{l-}(f)$ are mirrored:

$$H_{l-}(f) = H_{l+}(-f) \qquad (2)$$

and they overlap to form an "interference region", defined by $|f| \le W_i$, which is essential to achieving phase lock in the receiver's recombination of the split bands.

Section IV demonstrates that larger values of the interference region width $2W_i$ provide a better phase lock. However, we require:

$$f_s \geq W_i + W_g \tag{3}$$

where W_g is the bandwidth of the desired gap; thus, the larger we make W_i, the greater the extra bandwidth taken up by the TTIB signal.

If we further constrain the filters by making the frequency responses $H_{1\pm}(f)$ real, then a real input signal v(t) results in a real transmitted signal z(t). Thus the technique can be employed in a baseband data system to create a gap centered on 0 Hz in order to avoid distortion in ac coupling circuits.

The implementation appears difficult. However, for data signals we can make f_s a rational submultiple of the symbol rate, and precalculate all transmitted waveforms, including both the basic pulse shape and the TTIB effects. Modulation then becomes a matter of table lookup, as it is in most DSP based modems.

Channel Effects

The analysis below deals with static channels only. However, amplitude fading effects are considered in Section VI, and shown to have little effect on the results.

Processing in the pilot tone calibration subsystem is well known [1,3,4]. We assume that the combined effects of the channel and the pilot tone processing can be represented by a slowly varying residual carrier phase shift $\psi(t)$ and additive complex Gaussian noise with flat power spectrum N_o:

$$r(t) = e^{j\psi} z(t) + n(t) \tag{4}$$

Receiver Processing

As shown in Figure 4, the receiver recombines the signal bands by shifting the received complex envelope r(t) with complex carriers at $\pm f_s$, and passing the result through filters $H^*_{1+}(f)$ and $H^*_{1-}(f)$ which are matched to the transmitter's band split filters. In the case of data signals, these bandpass filters also include matching to the transmitted signal pulse. We define the combined transmitter and receiver filters as:

$$H_+(f) = |H_{1+}(f)|^2 \quad \text{and} \quad H_-(f) = |H_{1-}(f)|^2 \tag{5}$$

The filters $H_+(f)$ and $H_-(f)$ are designed with vestigial sideband symmetry:

$$H_+(f) + H_-(f) = 1 \quad \text{and} \quad H_+(f) = H_-(-f) \tag{6}$$

The shape of the rolloff through the interference region is not critical, though it can be selected to minimize the length of the impulse responses.

The local oscillator in Figure 4 has phase $\phi(t)$ with respect to the incoming carrier. Its variation is extremely slow compared with the signal v(t); if f_s is about 200 Hz, and the crystals controlling the oscillator have stability 10^{-4}, then $\phi(t)$ changes by 2π radians over 50 seconds. We also assume that $\psi(t)$ varies slowly compared with v(t), so that we can approximate the filter outputs as:

$$\begin{aligned} R_+(f) &= e^{j(\psi+\phi)}V_+(f) + N_+(f) \\ R_-(f) &= e^{j(\psi-\phi)}V_-(f) + N_-(f) \end{aligned} \tag{7}$$

where:

$$\begin{aligned} V_+(f) &= V(f)H_+(f) \\ N_+(f) &= N(f)H_{1+}^*(f) \end{aligned} \tag{8}$$

Definitions for $R_-(f)$, $V_-(f)$ and $N_-(f)$ are similar. In (8) we have ignored the phase rotation $\psi+\phi$ in the noise because of its circular symmetry.

The reconstructed signal $r_c(t)$ is formed by phase correcting $r_+(t)$ and $r_-(t)$ and summing them:

$$r_c(t) = r_+(t)e^{-j\hat{\phi}} + r_-(t)e^{j\hat{\phi}} \tag{9}$$

where $\hat{\phi}$ is an estimate of the local oscillator phase ϕ, obtained by techniques described in Sections III and IV. Substitution of 7,(8) gives:

$$R_c(f) = e^{j\psi}\left(e^{j\phi_e}H_+(f) + e^{-j\phi_e}H_-(f)\right)V(f) + N_c(f) \tag{10}$$

where the recombination phase errror $\phi_e = \phi - \hat{\phi}$. Since $n_+(t)$ and $n_-(t)$ are drawn from non-overlapping regions of the spectrum, they are independent, with power spectra $N_oH_+(f)$ and $N_oH_-(f)$, respectively. From the symmetry condition (6), the process $n_c(t)$ is white noise with power spectrum N_o. Again from (6), if the recombination phase error ϕ_e in (10) is zero, then there is no signal distortion. The carrier phase error ψ (and any channel amplitude fluctuation) propagates through to

$r_c(t)$ and must be tracked separately.

Effect of Recombination Phase Error

Now we examine the effect of non-zero recombination phase error ϕ_e. From (10) we see that the overall distortion is equivalent to a composite linear filter:

$$H_c(f) = e^{j\phi_e} H_+(f) + e^{-j\phi_e} H_-(f)$$

$$= \cos\phi_e + j\big(2H_+(f)-1\big)\sin\phi_e \qquad (11)$$

after substitution of (6). Note that $H_c(f)$ is conjugate symmetric, so the corresponding impulse response is real. Thus the real and imaginary components of the information signal v(t) are distorted independently in the same way, with no cross talk when the residual carrier phase shift ψ is zero. As an example, if the filter $H_+(f)$ has a raised cosine rolloff:

$$H_+(f) = \begin{cases} 0 & f<-W_i \\ \big(1 + \sin(\pi f/2W_i)\big)/2 & |f|\le W_i \\ 1 & f>W_i \end{cases} \qquad (12)$$

then the composite impulse response is real, and given by:

$$h_c(t) = \cos(\phi_e)\delta(t) - \sin(\phi_e)\big(\mathrm{sinc}(2W_i t+1/2)+\mathrm{sinc}(2W_i t-1/2)\big)/4t \qquad (13)$$

where $\delta(t)$ is the unit impulse function.

How severe is the distortion when applied to a data signal? Appendix A derives the sampled impulse response for a data system using spectral raised cosine pulses over a TTIB link with raised cosine rolloff in the filters $H_{\pm}(f)$. It demonstrates that non-zero values of reconstruction phase error ϕ_e result in loss of energy in the main component (the $\cos\phi_e$ term in (11) and (13)), as well as intersymbol interference. We can evaluate the effect on BER by explicitly calculating the probability of error for each pattern of neighbouring symbols, and averaging over all patterns. Figure 5 shows the result for coherent detection of 25% rolloff pulses, with symbol sequences truncated to 17 symbols, 8 on each side of the desired one. The

fractional interference width $T_s W_i$ has the value 0.05 in the Figure. However, it was found to have little effect on the error rate for a given ϕ_e. It is clear from the Figure that ϕ_e must be kept to values on the order of 0.1 radian or less to avoid excessive degradation. The losses are due almost entirely to intersymbol interference, rather than the reduced energy in the main component.

III RECOMBINATION PHASE LOCKING

Phase Detector

In order to bring the recombination phase error ϕ_e to zero, the receiver has to be able to measure it. Figure 4 illustrates the new symmetric phase detector [7]. We define the phase detector filters $\tilde{H}_{1+}(f)$ and $\tilde{H}_{1-}(f)$ as lowpassed versions of the transmitter's band splitting filters $H_{1+}(f)$ and $H_{1-}(f)$:

$$\tilde{H}_{1\pm}(f) = \begin{cases} H_{1\pm}(f), & |f| \le W_i \\ 0, & \text{elsewhere} \end{cases} \tag{14}$$

They are illustrated in Figure 6 for the special case of linear rolloff of $H_{\pm}(f)$ in the interference region.

Because we place $\tilde{H}_{1-}(f)$ in the positive branch, and $\tilde{H}_{1+}(f)$ in the negative branch, the composite transmitter and receiver filters in the two branches are identical, and given by:

$$H_o(f) = \tilde{H}_{1-}(f)\,\tilde{H}_{1+}(f) \tag{15}$$

The filter outputs $r_{2+}(t)$ and $r_{2-}(t)$ therefore contain the same signal component, and can be written:

$$r_{2\pm}(t) = e^{j(\psi\pm\phi)}v_2(t) + n_{2\pm}(t) \tag{16}$$

The common signal component is given by:

$$v_2(t) = \int v(t-\alpha)h_o(\alpha)d\alpha \tag{17}$$

and has autocorrelation function:

$$R_{v2}(\tau) = \frac{1}{2}\,E[v_2(t)v_2^*(t-\tau)] = \iint h_o^*(\alpha)h_o(\beta)R_v(\tau+\alpha-\beta)d\alpha d\beta \tag{18}$$

and power spectrum:

$$S_{v2}(f) = |H_o(f)|^2 S_v(f) \tag{19}$$

where $R_v(\tau)$ and $S_v(f)$ are the autocorrelation function and power spectrum of $v(t)$. We will assume that $S_v(f)$ is even over $|f| \le W_i$, so that both $R_{v2}(\tau)$ and $S_{v2}(f)$ are real and even.

The noise components $n_{2+}(t)$ and $n_{2-}(t)$ in (16) are independent,

because they are drawn from non-overlapping regions of the channel noise spectrum. Their power spectra and autocorrelation functions are given by:

$$S_{n2\pm}(f) = N_o \, |\tilde{H}_{1\mp}(f)|^2 = N_o \tilde{H}_{\mp}(f)$$

$$R_{n2\pm}(\tau) = \frac{1}{2} E[n_{2\pm}(t) n^*_{2\pm}(t-\tau)] = N_o \tilde{h}_{\mp}(\tau) \qquad (20)$$

where $\tilde{H}_{\pm}(f)$ denotes the filters $H_{\pm}(f)$ lowpassed to W_i, and $\tilde{h}_{\pm}(t)$ are the corresponding impulse responses. Note that the subscript sign reversal in (20) simply indicates that $n_+(t)$ has most of its power in negative frequencies (vice versa for $n_-(t)$). The following symmetries are useful in later analysis:

$$R_{n2\pm}(-\tau) = R^*_{n2\pm}(\tau) = R_{n2\mp}(\tau) \qquad (21)$$

Phase detection is accomplished by the basic operation:

$$e(t) = r_{2+}(t) r^*_{2-}(t) \qquad (22)$$

In the absence of channel noise, we see by substitution of (16) that:

$$e(t) = e^{j2\phi} \, |v_2(t)|^2 \qquad (23)$$

Since the phase of e(t) is at all times given by 2ϕ, there is no self noise. Availability of this phase error signal requires only that v(t) have energy in $|f| \leq W_i$; it does not depend on whether v(t) is speech or data.

The use of symmetric filters to eliminate self noise was first identified in [7]. The phase detector presented here is an improvement in two respects: its filters are simpler in form and simpler to analyse, and it gives 0.3 dB better jitter performance. In general, the phase detector filters $\tilde{H}_{1+}(f)$ and $\tilde{H}_{1-}(f)$ can be cascaded with any filter $H_3(f)$ inserted in both branches. In [7], for example, the filtering is equivalent to $H_3(f) = H^*_o(f)$. We experimented numerically, using the techniques developed in Section IV, with such filters, setting the magnitude response to a power of that of $H_o(f)$. We found that the lowest jitter was obtained with a flat frequency response; that is, with $H_3(f)$ absent.

Since (23) depends on 2ϕ, there is a two-fold ambiguity in the phase detector, which forces the use of differential encoding in the

data stream. Normally, we do not consider this to be a problem, as it merely doubles the bit error rate. In fading channels, however, BER decreases inversely with SNR. Therefore phase locked TTIB costs 3 dB in comparison with other pilot tone based systems, which are supposed not to need differential encoding.

Feedforward Phase Tracking

The phase error signal (22) is noisy. The fluctuations about the true phase ϕ induced by channel noise are, in a sense, amplified by the inherent variability of $|v(t)|^2$. Although it is possible to smooth the variations directly with a phase locked loop, it is better to reduce the larger phase swings by preceding the loop with a lowpass filter. We have modelled the averaging as taking place entirely within the lowpass filter, and have left the loop only the job of phase halving. In fact, the use of a loop is simply to provide phase continuity; the alternative method of direct mathematical halving of the angle of $e_4(t)$ can cause phase reversals in the correction waveform $\exp(j\hat{\phi})$, and hence in the output $r_c(t)$.

The feedforward structure permits a great deal of flexibility. For example, we could replace the lowpass filter with an infinite memory block averager, and force the phase error to zero. Normally, though, we allow for drift in the transmitter oscillator and use a "lossy integrator"; that is, a lowpass filter with finite dc gain.

It is also possible to track the phase with a feedback structure. Simply replace the local oscillator in Figure 4 with a VCO having f_s as its free running frequency, and control its instantaneous frequency with Im[e(t)] or arg[e(t)]. For small phase error values, a linearized model is appropriate, and performance is the same as that of the feedforward tracker.

IV RECOMBINATION PHASE JITTER

Earlier we examined the phase locking structure and the effect of recombination phase error ϕ_e on the bit error rate. In this section, we obtain the variance and the pdf of ϕ_e.

First, substitute (16) into (22), and group terms in the phase detector output as follows:

$$e(t) = e^{j2\phi} \left(\mu + \nu(t) + \eta(t)\right) \tag{24}$$

where μ is the mean value over the noise and data ensembles, and $\nu(t)$ is real, representing the fluctuations in the data squared term:

$$\nu(t) = |v_2(t)|^2 - \mu \tag{25}$$

The remaining noise $\eta(t)$ is complex, and depends on both signal and noise fluctuations:

$$\eta(t) = e^{j(\psi-\phi)} v_2(t) n_{2-}^*(t) + e^{-j(\psi+\phi)} v_2^*(t) n_{2+}(t) + e^{-j2\phi} n_{2+}(t) n_{2-}^*(t) \tag{26}$$

Note that since the processes $v_2(t)$, $n_{2+}(t)$ and $n_{2-}(t)$ are independent and zero mean, the processes $\nu(t)$ and $\eta(t)$ are uncorrelated and zero mean.

The statistics of each term in (24) and the resulting jitter statistics are developed below.

Mean Value

The mean value μ in $e(t)$ depends only on the data signal, since the channel noise contribution $\eta(t)$ has a zero mean. Take the expectation of (23):

$$\mu = E[e^{-j2\phi}\, e(t)] = E[|v_2(t)|^2] = 2\, R_{v2}(0) \tag{27}$$

Since $R_{v2}(\tau)$ is real, so is μ.

Statistics of the Real Noise Term

We need the second order statistics of the real noise $\nu(t)$. Its autocorrelation function can be written:

$$R_\nu(\tau) = E[\nu(t)\nu(t-\tau)] = E[|v_2(t)|^2 |v_2(t-\tau)|^2] - \mu^2 \tag{28}$$

Substitute (17), and write:

$$R_\nu(\tau) + \mu^2 = \iiiint h_o(\alpha)h_o^*(\beta)h_o^*(\gamma)h_o(\delta)$$
$$\cdot E[v(t-\alpha)v^*(t-\beta)v^*(t-\tau-\gamma)v(t-\tau-\delta)]d\alpha\, d\beta\, d\gamma\, d\delta \qquad (29)$$

Because of the lowpass nature of $h_o(t)$, we can replace $v(t)$ in (29) with its lowpassed equivalent. From the central limit theorem, $v(t)$ when lowpassed to W_1 is Gaussian, to a good approximation. Now we can make use of a result on high order joint moments of Gaussian random variables [8] to write the expectation in the integrand of (29) as:

$$4R_v(\beta-\alpha)R_v(\delta-\gamma) + 4R_v(\tau+\gamma-\alpha)R_v(\tau+\delta-\beta) \qquad (30)$$

Substituting into (29) and making use of the fact that $|H_o(f)|^2$ is even gives us the desired result:

$$R_\nu(\tau) = 4R_{v2}^2(\tau) \qquad (31)$$

Since $R_{v2}(\tau)$ is real and even, so is $R_\nu(\tau)$.

In the frequency domain, we have the convolution relation:

$$S_\nu(f) = 4\int S_{v2}(f-\xi)S_{v2}(\xi)d\xi \qquad (32)$$

Statistics of the Complex Noise Term

The complex noise $\eta(t)$ in (26) is the source of the error in estimating ϕ; if its imaginary part were zero, then feedforward recombination would be perfect at all times. A few observations make obtaining its second order statistics straightforward. First, the three terms in (26) are uncorrelated (though not independent), because the three underlying processes $v_2(t)$, $n_{2+}(t)$ and $n_{2-}(t)$ are independent and zero mean. We can therefore calculate the autocorrelation function of each term separately. Second, $\eta(t)$ is circularly symmetric:

$$E[\eta(t)\eta(t-\tau)] = 0 \qquad (33)$$

so its real and imaginary parts have the same statistics, and we can ignore the phase rotations ψ and ϕ. The autocorrelation of $\eta(t)$ can therefore be written:

$$R_\eta(\tau) = \frac{1}{2}\, E[\eta(t)\eta^*(t-\tau)]$$

$$- \frac{1}{2} E[v_2(t)v_2^*(t-\tau)n_{2-}^*(t)n_{2-}(t-\tau)] + \frac{1}{2} E[v_2^*(t)v_2(t-\tau)n_{2+}(t)n_{2+}^*(t-\tau)]$$

$$+ \frac{1}{2} E[n_{2+}(t)n_{2+}^*(t-\tau)n_{2-}^*(t)n_{2-}(t-\tau)] \quad (34)$$

Since signal and noise are independent:

$$R_\eta(\tau) = 2R_{v2}(\tau)R_{n2-}^*(\tau) + 2R_{v2}^*(\tau)R_{n2+}(\tau) + 2R_{n2+}(\tau)R_{n2-}^*(\tau) \quad (35)$$

We use the symmetry conditions (21) and the fact that $R_{v2}(\tau)$ is real to obtain:

$$R_\eta(\tau) = 4R_{v2}(\tau)R_{n2+}(\tau) + 2R_{n2+}^2(\tau) \quad (36)$$

The corresponding power spectrum is:

$$S_\eta(f) = 4N_o\int S_v(\xi)|H_o(\xi)|^2\tilde{H}_-(f-\xi)d\xi + 2N_o^2\int|\tilde{H}_-(\xi)|^2\tilde{H}_-(f-\xi)d\xi \quad (37)$$

It is clear that the power spectrum $S_\eta(f)$, though real, is asymmetric, with most of the power in the negative frequencies. This simply means that the process $\eta(t)$ has a tendency to rotate in the mathematically negative direction. However, the real and imaginary components $\eta_r(t)$ and $\eta_i(t)$ of $\eta(t)$ share the same even power spectrum, which we denote by $S_{\eta r}(f)$:

$$S_{\eta r}(f) = \frac{1}{2}\left(S_\eta(f)+S_\eta(-f)\right) \quad (38)$$

Probability Density Function of Phase Error

The lowpass filter which precedes the phase halving loop has frequency response $H_L(f)$, with unity dc gain and noise bandwidth W_L. Its output can be written:

$$e_4(t) = e^{j2\phi}\left(\mu + \nu_4(t) + \eta_4(t)\right) \quad (39)$$

where $\nu_4(t)$ and $\eta_4(t)$ are lowpassed versions of $\nu(t)$ and $\eta(t)$. The variances of the real and imaginary components of $e_4(t)$ differ:

$$\sigma_{4i}^2 = \int|H_L(f)|^2S_{\eta r}(f)df$$

$$\sigma_{4r}^2 = \sigma_{4i}^2 + \int|H_L(f)|^2S_\nu(f)df \quad (40)$$

The phase at this point:

$$\phi_4 = \arg\left(\mu + \nu_4(t) + \eta_4(t)\right) \tag{41}$$

is related to the overall phase error ϕ_e by reduction modulo 2π:

$$\phi_4 = (2\phi_e) \bmod 2\pi \tag{42}$$

The relation between probability density functions of such phase variables is discussed in detail in [4]. Here we simply obtain the pdf of ϕ_4 and approximate the variance of ϕ_e.

Earlier we approximated $v_2(t)$ as Gaussian, on the grounds that the long memory of the lowpass phase detection filters averaged many independent samples. By the same argument, but with perhaps less justification, we approximate the lowpass filter outputs $\nu_4(t)$ and $\eta_4(t)$ as Gaussian. Now we can make use of a standard result [9, p 167], modified to account for unequal variances in the real and imaginary parts. Define:

$$\epsilon = \sigma_{4r}/\sigma_{4i}$$

$$\gamma = \mu^2/\sigma_{4r}^2$$

$$\alpha^2(\phi_4) = \frac{\gamma}{1 + \epsilon^2\tan^2(\phi_4)} \tag{43}$$

and the probability density function of ϕ_4 is given by:

$$p(\phi_4) = \frac{e^{-\gamma/2}}{2\pi} \frac{\epsilon}{\cos^2(\phi_4)+\epsilon^2\sin^2(\phi_4)} \left[1 + \sqrt{2\pi}\,\alpha(\phi_4)e^{\alpha^2(\phi_4)/2}Q\left(-\alpha(\phi_4)\right)\right] \tag{44}$$

Phase Error Variance

The pdf of ϕ_4 (44) is more interesting than useful. However, we can approximate the mean square recombination phase error quite well when it is small, without requiring the filter output to be Gaussian. From (41) and (42) we have:

$$\phi_e(t) \approx \frac{1}{2} \frac{\eta_{4i}(t)}{\mu + \nu_4(t) + \eta_{4r}(t)}$$

$$\approx \frac{1}{2} \frac{\eta_{4i}(t)}{\mu} \left(1 - \frac{\nu_4(t) + \eta_{4r}(t)}{\mu}\right) \tag{45}$$

Since all the noise components are independent, we have the approximate jitter variance:

$$\sigma_{\phi e}^2 \simeq \frac{1}{4}\frac{\sigma_{4i}^2}{\mu^2}\left(1+\frac{\sigma_{4r}^2}{\mu^2}\right)$$

$$= \frac{1+\gamma}{4\epsilon^2\gamma^2} \tag{46}$$

V FILTERS WITH LINEAR ROLLOFF

We are now in a position to apply the general results of Section IV to a specific PLTTIB system which, though simplified in some respects, is still representative.

Linear Rolloff Filters and Signal Power Spectrum

We assume the use of band splitting filters $H_{1\pm}(f)$ for which the vestigial symmetry (6) has a linear rolloff in the interference region, as shown in Figure 6. Thus:

$$\tilde{H}_{\pm}(f) = \begin{cases} \frac{1}{2}(1 \pm f/W_i), & |f| \le W_i \\ 0, & \text{elsewhere} \end{cases} \tag{47}$$

and:

$$|H_o(f)|^2 = \frac{1}{4}\left(1 - (f/W_i)^2\right) \tag{48}$$

Our second simplifying assumption is that the power spectrum $S_v(f)$ of the signal is flat over the bandwidth of the filter:

$$S_v(f) = S_o \tag{49}$$

For a PLTTIB data system, this is a reasonable assumption. In fact, for signalling with spectral raised cosine pulses, S_o equals E_s, the energy per symbol. In voice PLTTIB systems, the assumption is a little more suspect, since there are formant peaks in the speech power spectrum.

Taken together, the two assumptions simplify the key power spectrum $S_{v2}(f)$ (19):

$$S_{v2}(f) = S_o\left(1 - (f/W_i)^2\right)/4, \qquad |f| \le W_i \tag{50}$$

Mean Value

The mean value μ of the phase detector output is easily obtained. From (27) and (50), we have:

$$\mu = 2\int_{-W_i}^{W_i} S_{v2}(f)\, df = \frac{2}{3} S_o W_i \tag{51}$$

Spectrum of the Real Noise

The power spectrum $S_\nu(f)$ of the real noise component of the phase detector output follows from (32) and (50):

$$S_\nu(f) = 4\, S_o^2 \int_{-W_i+|f/2|}^{W_i-|f/2|} |H_o(\tfrac{f}{2} - \xi)|^2\, |H_o(\tfrac{f}{2} + \xi)|^2\, d\xi \qquad (52)$$

where the convolution has been written in a symmetric form to simplify the result. Substitution of (48) and subsequent manipulation give:

$$S_\nu(u) = \frac{S_o^2 W_i}{2} \left\{(1-u^2)^2(1-|u|) - \tfrac{2}{3}(1+u^2)(1-|u|)^3 + \tfrac{1}{5}(1-|u|)^5\right\} \qquad (53)$$

where u is normalized frequency:

$$u = f/2W_i \qquad (54)$$

Clearly, $S_\nu(f)$ is symmetric, though it has a slope discontinuity at f=0.

Spectrum of the Complex Noise

The spectrum $S_\eta(f)$ of the complex noise component of the phase detector output can be obtained from (37) in a similar fashion. Substituting (47-49) and carrying out the convolutions yields:

$$S_\eta(u) = N_o S_o W_i \left((1-u-u^2+u^3)(1-|u|) - \tfrac{1}{3}(1+u)(1-|u|)^3\right) + N_o^2 W_i (1-|u|)\left((1-u)^2 - \tfrac{1}{3}(1-|u|)^2\right) \qquad (55)$$

which is asymmetric, and has a slope discontinuity at f=0.

Figure 7 presents the two spectra, $S_\nu(f)$ and $S_\eta(f)$, normalized by division by $S_o^2 W_i$. The parameter Γ_o is the SNR:

$$\Gamma_o = S_o/N_o \qquad (56)$$

The asymmetry is clearly evident. Also presented is $S_{\eta r}(f)$, the spectrum of the real and imaginary components of $\eta(t)$, which from (38) is the even part of $S_\eta(f)$. Its slope discontinuity is negligible.

Mean Square Recombination Phase Error

The output of the lowpass filter, as we have seen, has unequal variances in the radial and tangential directions. Exact calculation requires substitution of (53), (55) and (38) into (40) and evaluation of the integrals. Figure 8 illustrates the result for the case of an ideal rectangular lowpass filter, and shows how the bandwidth ratio W_L/W_i and the SNR Γ_o can be traded off when the variance $\sigma^2_{\phi e}$ is fixed. The three values of the variance parameter $\sigma^2_{\phi e}$ were selected to put $\phi_e = 0.1$ rad (which we determined earlier as a reasonable upper limit) at 1, 2, and 3 standard deviations from zero.

A simple approximation gives more insight into the effects of the various parameters. We assume that the bandwidth W_L of the lowpass is small, in order to keep the phase jitter small. We can then approximate the power spectra $S_\nu(f)$ and $S_{\eta r}(f)$ over the filter passband as flat with values $S_\nu(0)$ and $S_{\eta r}(0)$, respectively, and obtain:

$$\sigma^2_{4i} \approx \frac{4}{3} N_o W_i W_L (S_o + N_o)$$

$$\sigma^2_{4r} = \frac{4}{3} W_i W_L \left(\frac{2}{5} S_o^2 + S_o N_o + N_o^2 \right) \qquad (57)$$

Figure 7 gives a visual indication of the quality of the approximation; it is increasingly pessimistic as W_L increases. In practice, the error in σ^2_{4i} is small over useful ranges of W_L/W_i and Γ_o. Since $S_\nu(f)$ is narrower, the error in σ^2_{4r} is larger, especially at lower SNR. However, for $\Gamma_o > 10$ and $W_L < 0.2\ W_i$, the error in $\sigma^2_{\phi e}$ is less than 5%. In any case, the approximation is not critical, since it is intended only as a way to generate simplified anlytical results, and it can be improved by higher order polynomial fits, or by explicit numerical integration.

The parameters (43) of the pdf of the phase error ϕ_4 at the filter output ϕ_4 are given relatively simply by:

$$\epsilon^2 = \frac{\frac{2}{5}\Gamma_o^2 + \Gamma_o + 1}{\Gamma_o + 1}$$

$$\gamma = \frac{1}{3}\frac{W_i}{W_L}\frac{\Gamma_o^2}{\frac{2}{5}\Gamma_o^2 + \Gamma_o + 1} \qquad (58)$$

Finally, we have the approximate variance of the recombination phase error ϕ_e from (46):

$$\sigma^2_{\phi e} \simeq \frac{3}{4}\frac{W_L}{W_i}\frac{\Gamma_o+1}{\Gamma_o^2}\left(1+\frac{3W_L}{W_i}\left(\frac{2}{5}+\Gamma_o^{-1}+\Gamma_o^{-2}\right)\right) \tag{59}$$

and if the SNR Γ_o is large compared to one, then:

$$\sigma^2_{\phi e} \simeq \frac{3}{4}\frac{W_L}{W_i}\frac{1}{\Gamma_o}\left(1+\frac{2}{5}\frac{W_L}{W_i}\right) \tag{60}$$

From (59) and (60), the jitter can be reduced by increasing W_i, the width of the overlap region. As noted earlier, though, the bandwidth occupied by the transmitted signal then increases. In any case, W_i can be no greater than the original signal bandwidth.

Acquisition Time

We can make the mean square recombination phase error as small as desired simply by decreasing the lowpass filter bandwidth. However, this is at the expense of acquisition time. We can estimate the acquisition time as about three "time constants" of the lowpass filter, which we in turn estimate from its noise bandwidth:

$$T_a \simeq 3\tau_L \simeq 3/2\pi W_L \tag{61}$$

More useful is the number of symbols needed for acquisition. With a symbol rate R_s, the length of the acquisition sequence in symbols is given by:

$$N_a \simeq \frac{3R_s}{2\pi W_L} = \frac{3}{2\pi}\frac{R_s}{W_i}\left(\frac{W_L}{W_i}\right)^{-1} \tag{62}$$

We can determine the variation of required acquisition sequence length with SNR when jitter variance is fixed: solve the approximation (59) for W_L/W_i or use the exact results shown on Figure 8, and substitute in (62). The result for the exact calculation is shown in Figure 9, where we assume that W_i is 10% of the symbol rate R_s. If we set $\sigma^2_{\phi e} = 2.5\text{x}10^{-3}$ rad^2 (i.e. 0.1 rad is the 2σ point), then N_a is about 190 symbols at Γ_o = 10 dB. This is fairly long, though not excessive.

Finally, for very high SNR values, the phase error in the phase detector output e(t) may already be low enough not to require lowpass

filtering. In fact, for infinite SNR, acquisition is virtually instantaneous, since there is no self noise in a symmetric phase detector.

VI FADING CHANNELS

To this point the analysis has dealt only with static channels. For a realistic assessment, though, we must also consider behaviour of PLTTIB on fading channels. The argument below suggests that both recombination phase error variance and acquisition time are significantly improved for normal parameter ranges on such channels.

Deep fades are rare. For example, if a system is to be designed for an average BER of 10^{-3}, then it is well known [7] that for Rayleigh fading the average SNR should be on the order of 30 dB. Since the received power is exponentially distributed, the fraction of time occupied by fades taking the SNR down to 20 dB is only 10%, and to 10 dB is only 1%. We can easily freeze the phase halving loop when the SNR falls below some threshold, with the result that its behavior is determined only by the high SNR intervals, which make up most of the time. The bandwidth of the lowpass filter preceding the loop can also be increased, thereby shortening the acquisition time.

There remains one point concerning the analytical model in the presence of fading. From the development in Section II, we see that fading imparts a varying amplitude and phase ψ to the signal component of r(t) (4), though the noise level is unchanged. If we take these fluctuations into account, the assumption of slow variation in complex channel gain which led to (16) is no longer strictly valid, and there is more signal distortion than estimated in Section III. However, the phase and amplitude variations are relatively slow most of the time, and rapid fluctuations are normally associated with the infrequent deep fades. Thus the desired component e(t) of the phase detector output is given by (23) most of the time, though it is now proportional to the instantaneous value of signal power; and because the loop is frozen during deep fades, the intervals when (23) is not valid are prevented from affecting its operation.

We can conclude that phase jitter and acquisition time are significantly improved on fading channels, in comparison with static channels of the same BER.

VII CONCLUSIONS

TTIB creates a spectral gap by separating subbands with modulation. Coherent recombination of the subbands is essential to data transmission. This paper has presented a full analysis of several topics related to the recombination phase error, which should not be confused with the usual carrier phase error. The use of a symmetric phase detector for PLTTIB was assumed throughout.

One observation was the existence of a two-fold phase ambiguity, which forces the use of differential encoding, with a consequent 3 dB loss when used over fading channels. The effect of recombination phase error ϕ_e on BER performance was evaluated, and it was demonstrated that ϕ_e should be held to 0.1 radians or less if SNR degradation is not to exceed 1 dB.

Phase detection in PLTTIB depends on the properties of signal and noise in the interference region, the spectral overlap of the bandpass filters which define the subbands. The paper confirmed the result in [7] that symmetry in the phase detector filters elimiminates the self noise problem identified in [6]. It also demonstrated that simpler filters than those in [7] can provide somewhat lower phase jitter.

The general analysis presented the jitter variance and its approximate pdf for arbitrary filter shapes. More detailed results from the specific case of linear rolloff in the interference region showed that, not surprisingly, the jitter variance is inversely proportional to SNR in the interference region. It is also inversely proportional to the width of the interference region; however, improvement by increasing this region comes at the expense of increased channel bandwidth.

The phase jitter can, of course, be reduced by narrowing the bandwidth of the tracking filter, though this increases the acquisition time. At an SNR of 10 dB in the interference region, an acceptably low phase jitter requires an acquisition time of about 190 symbols. However, on a noise-free channel, PLTTIB with a symmetric phase detector can in principle acquire lock instantly, because of its elimination of self-noise,

Although the analysis was based on the assumption of a static channel, consideration of the properties of fading channels suggests that phase jitter and acquisition time are much improved in comparison

with static channels of the same BER.

APPENDIX A

ISI INTRODUCED BY PHASE ERROR

In this appendix we derive the sampled impulse response of a TTIB data system employing square root spectral raised cosine pulses. Denote the Fourier transform of the pulse by P(f). It satisfies:

$$|P(f)|^2 = \begin{cases} T_s & , \ |2T_s f| \le (1-r) \\ T_s \sin\left(\pi(1-2T_s f)/2r\right) & , \ (1-r) \le |2T_s f| \le (1+r) \\ 0 & , \ \text{elsewhere} \end{cases} \tag{A1}$$

where r is the rolloff factor and T_s is the symbol duration. The overall pulse shape $p_o(t)$ of the cascade of pulse shaping filter, TTIB distortion and matched filter therefore has the transform:

$$P_o(f) = H_c(f)|P(f)|^2 \tag{A2}$$

where $H_c(f)$ is the composite TTIB distortion filter (11). The overall sampled pulse response $p_o(kT_s)$, when convolved with the input data sequence, determines the signal values entering the decision device, and hence the level of intersysmbol interference.

Inverse transforming (A2) gives $p_o(kT_s)$:

$$p_o(kT_s) = \int_{-(1+r)/2T_s}^{(1+r)/2T_s} P_o(f) \exp(j2\pi fkT_s)\, df \tag{A3}$$

We evaluate by dividing the integration in (A3) into three regions: $|f| \le W_i$, $W_i \le |f| \le (1-r)/2T_s$, and $(1-r)//2T_s \le |f| \le (1+r)/2T_s$. The contribution $p_o(0)$ of the desired pulse is easily obtained as:

$$p_o(kT_s) = \cos(\phi), \quad k=0 \tag{A4}$$

regardless of the exact rolloff of the TTIB bandsplit filter. For the ISI contribution (i.e. $k \neq 0$) we assume a raised cosine rolloff of the TTIB filter as given in (12). After some algebra, we obtain:

$$\begin{aligned} p_o(kT_s) = \sin(\phi)\Big\{ & T_s W_i \left(\text{sinc}(1+4kT_s W_i) - \text{sinc}(1-4kT_s W_i)\right) \\ & + \left(\cos(\pi k(1-r)) - \cos(2\pi kT_s W_i)\right)/\pi k \\ & + (-1)^k 4kr^2 \cos(\pi kr)/\pi(1+2kr)(1-2kr)\Big\}, \quad k \neq 0 \end{aligned} \tag{A5}$$

We see from (A4) and (A5) that if the recombination phase error ϕ is zero, then the sampled impulse response $p_o(kT_s)$ has the value 1 for k=0,

and the value 0 for all other k. That is, there is no distortion. However, for nonzero values of ϕ, the energy in the desired term (A4) decreases as $\cos(\phi)$, while the intersymbol interference terms (A5) increase as $\sin(\phi)$.

REFERENCES

[1] A.J. Bateman et al, "Speech and Data Communications Over 942 MHz TAB and TTIB Single Sideband Mobile Radio Systems Incorporating Feed-Forward Signal Regeneration", IEEE Trans Vehicular Techn, vol vt-34, no 1, pp 13-21, February 1985.

[2] J.P. McGeehan and A.J. Bateman, "Phase Locked Transparent Tone-in-Band (TTIB): A New Spectrum Configuration Particularly Suited to the Transmission of Data Over SSB Mobile Radio Networks", IEEE Trans Commun, vol COM-32, no 1, pp 81-87, January 1984.

[3] F. Davarian, "Mobile Digital Communications via Tone Calibration", IEEE Trans Vehicular Techn, vol VT-36, pp 55-62, May 1987.

[4] M.K. Simon, "Dual-Pilot Tone Calibration Technique", IEEE Trans Vehicular Techn, vol VT-35, no 2, pp 63-70, May 1986.

[5] P.M. Martin et al, "The Implementation of a 16-QAM Mobile Data System Using TTIB-Based Fading Correction Techniques", IEEE Vehicular Techn Conf, pp 71-76, Philadelphia, 1988.

[6] J.K. Cavers, "An Analysis of Phase Locked Transparent Tone-in-Band", IEEE Vehicular Techn Conf, San Francisco, 1989.

[7] A. Bateman, "Feedforward Transparent Tone-in-Band: Its Implementation and Applications", submitted to IEEE Trans Vehicular Techn, January 1989.

[8] J.M. Wozencraft and I.M. Jacobs, Principles of Communication Engineering, pp 205-206, John Wiley, 1965.

[9] J.G. Proakis, Digital Communications, McGraw-Hill, 1983.

ILLUSTRATIONS

Figure 1 Functional Organization of PLTTIB System
Figure 2 TTIB Transmitter Processing
Figure 3 Spectra in PLTTIB
Figure 4 Phase Locked TTIB Receiver
Figure 5 Effect of Recombination Phase Error on BER
Figure 6 Phase Detector Filter With Linear Rolloff
Figure 7 Normalized Phase Detector Noise Power Spectra
Figure 8 Lowpass Bandwidth With Fixed Jitter Variance
Figure 9 Acquisition Time With Fixed Jitter Variance

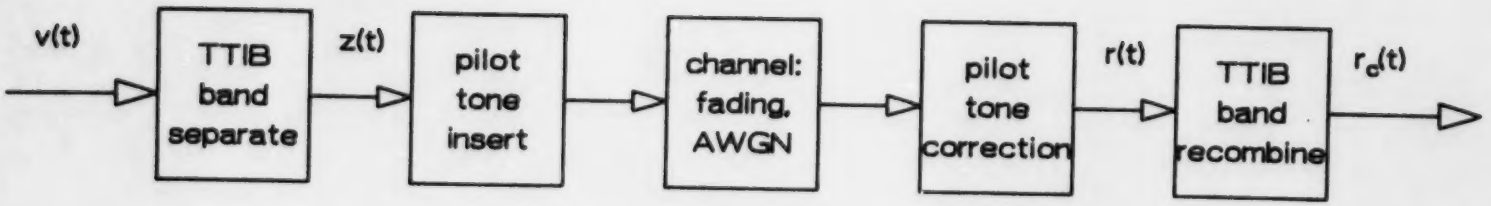

Figure 1 Functional Organization of PLTTIB System

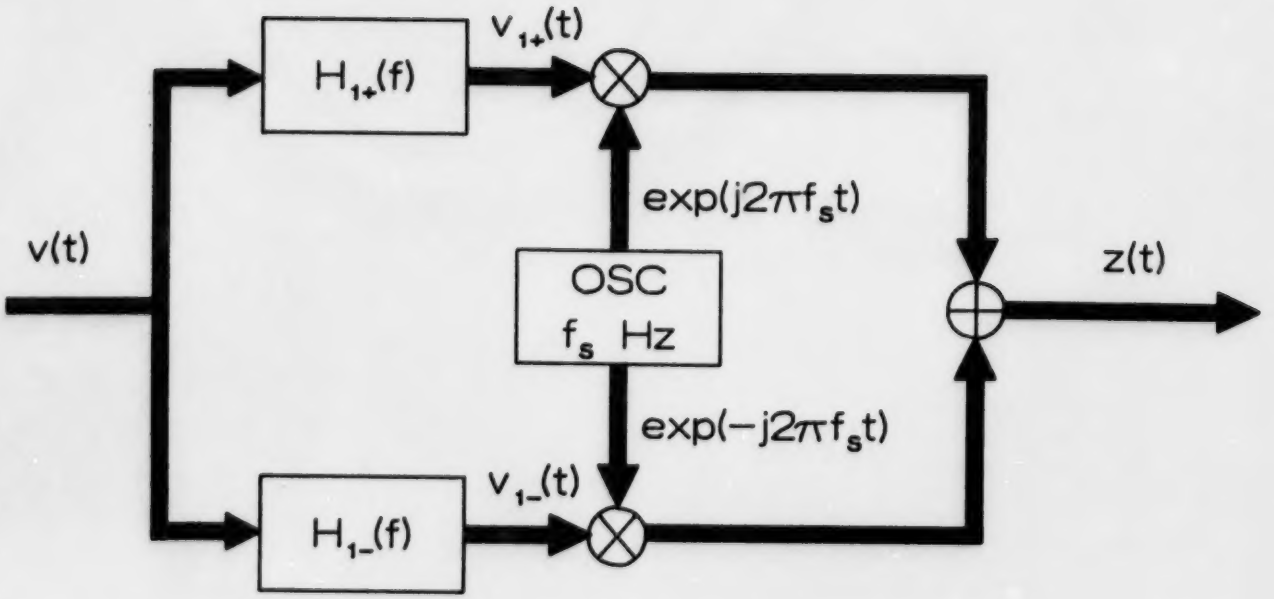

Figure 2 TTIB Transmitter Processing

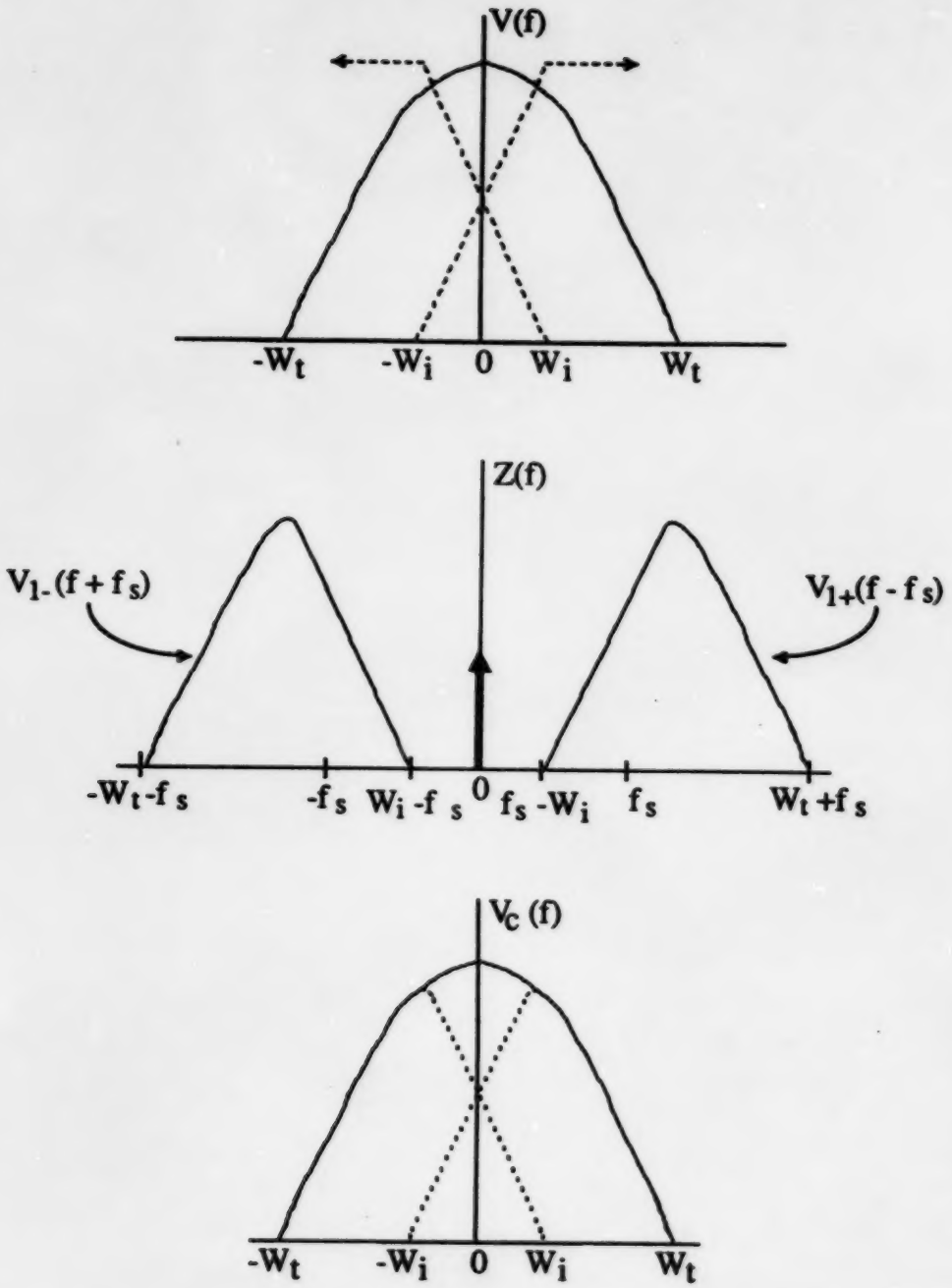

Figure 3 Spectra in PLTTIB

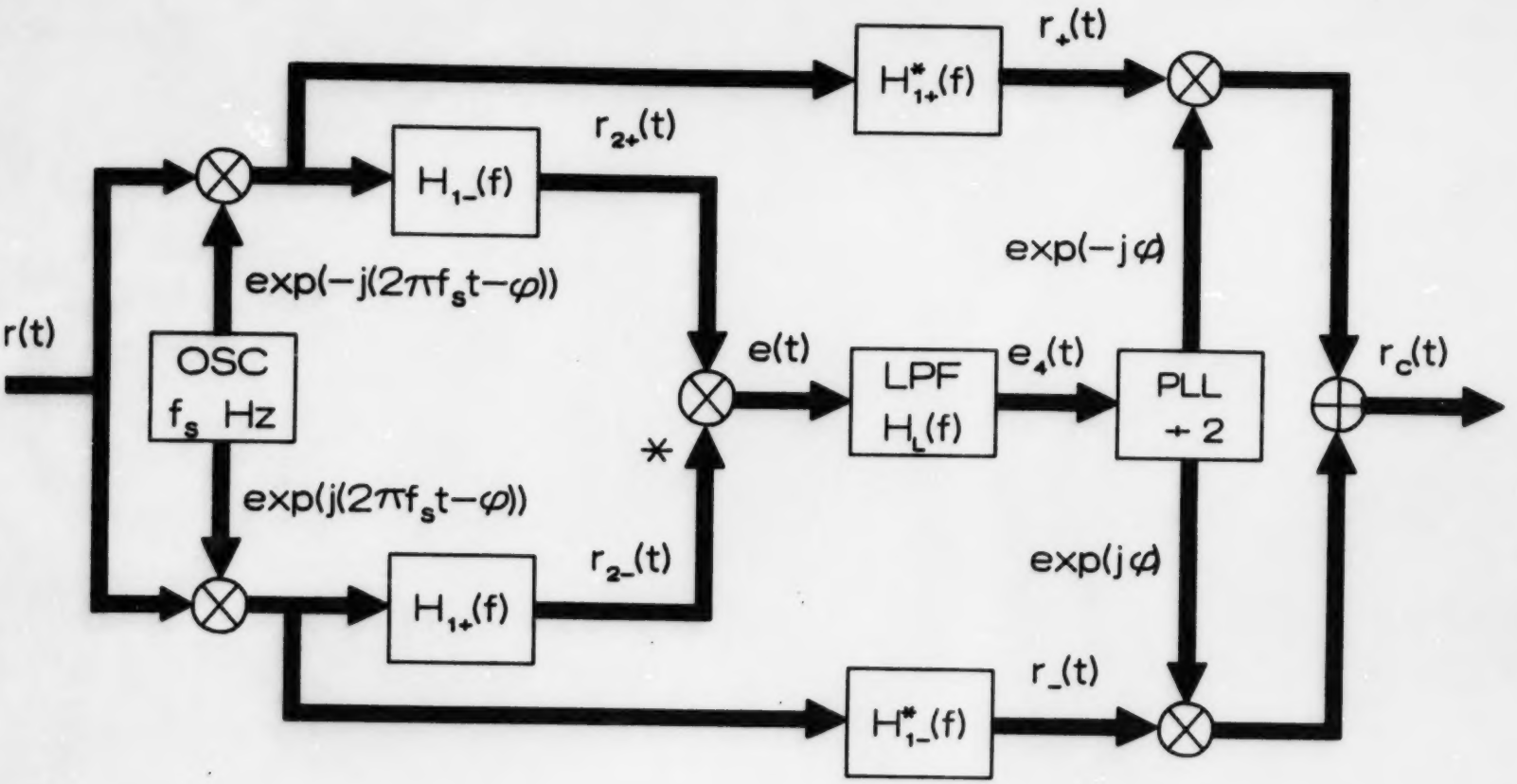

Figure 4 Phase Locked TTIB Receiver

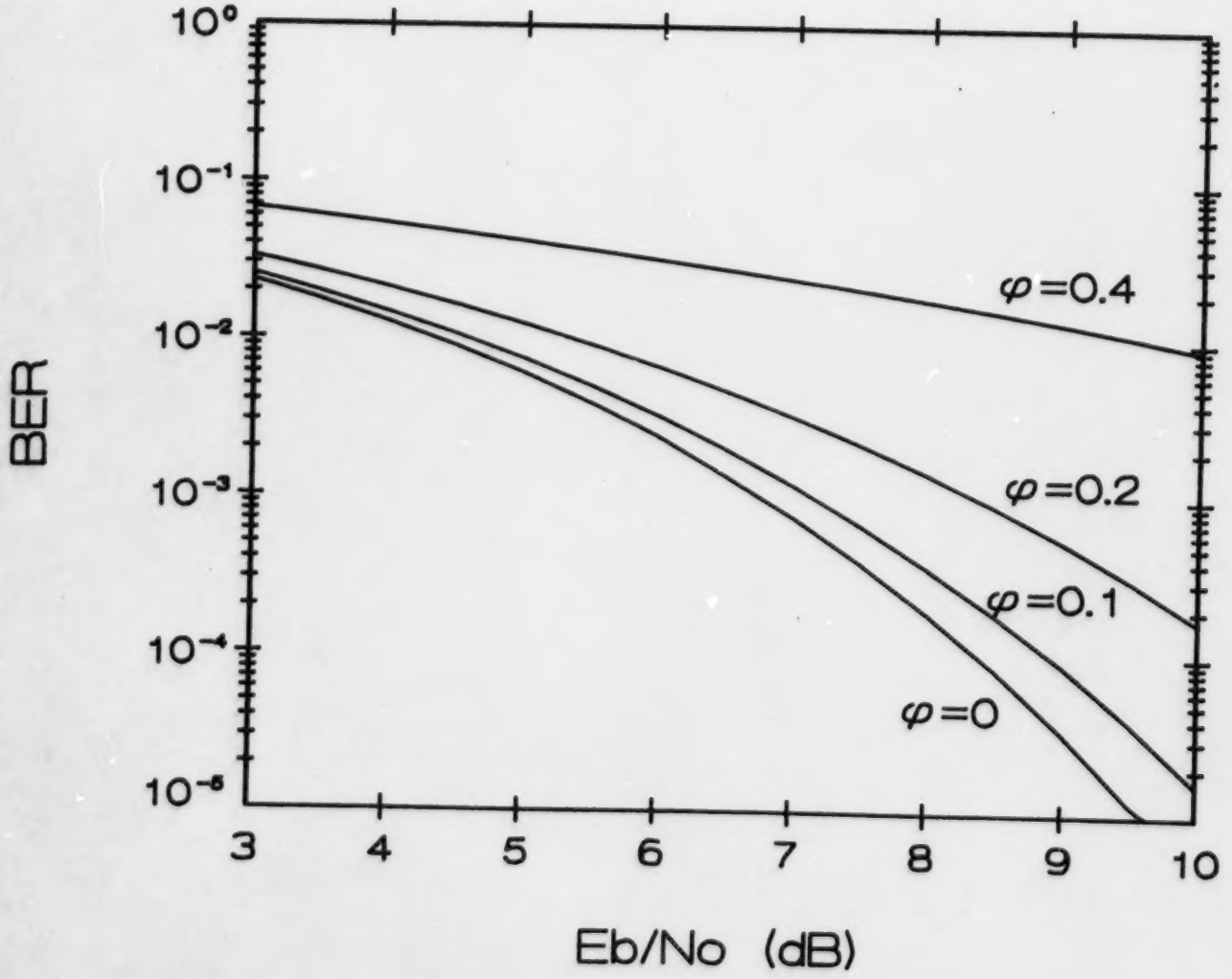

Figure 5 Effect of Recombination Phase Error on BER

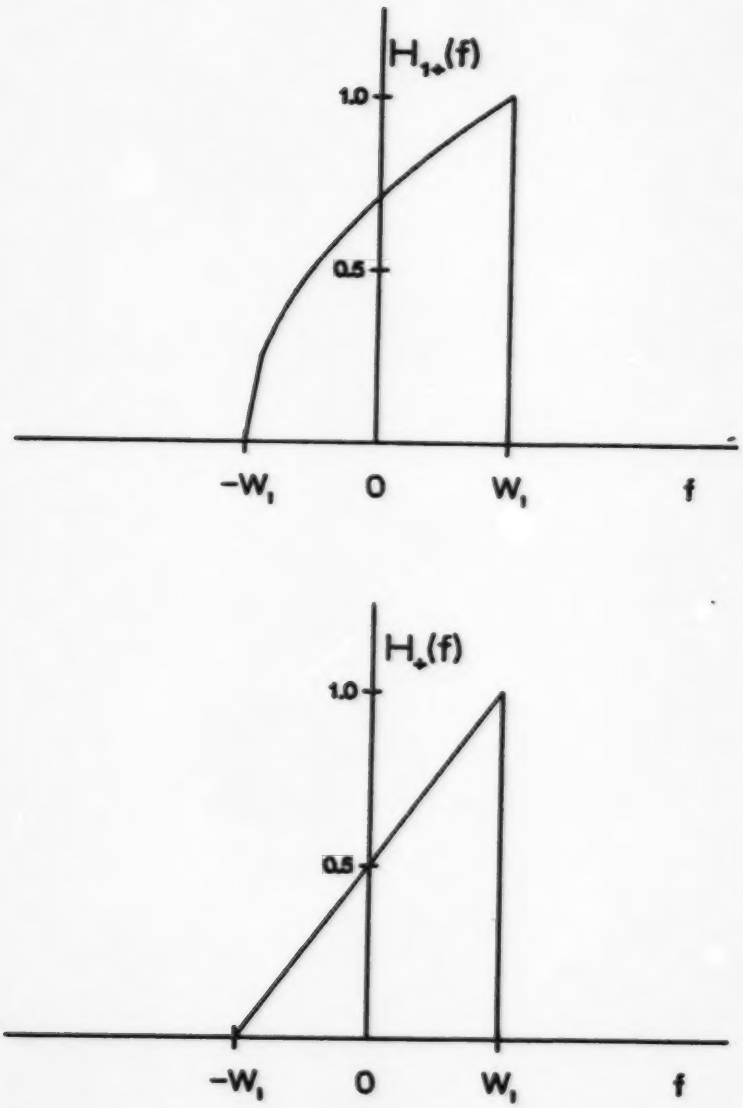

Figure 6 Phase Detector Filter With Linear Rolloff

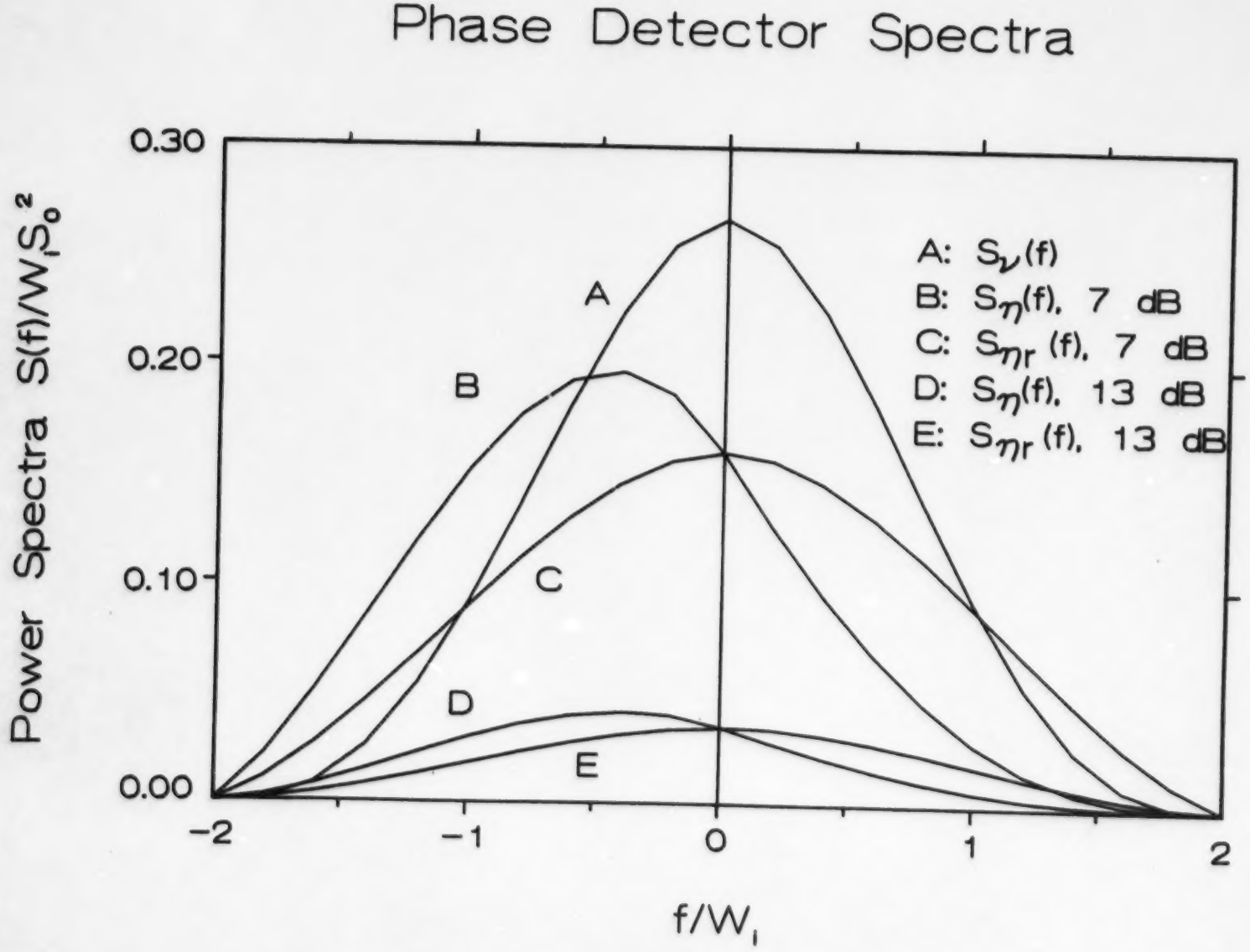

Figure 7 Normalized Phase Detector Noise Power Spectra

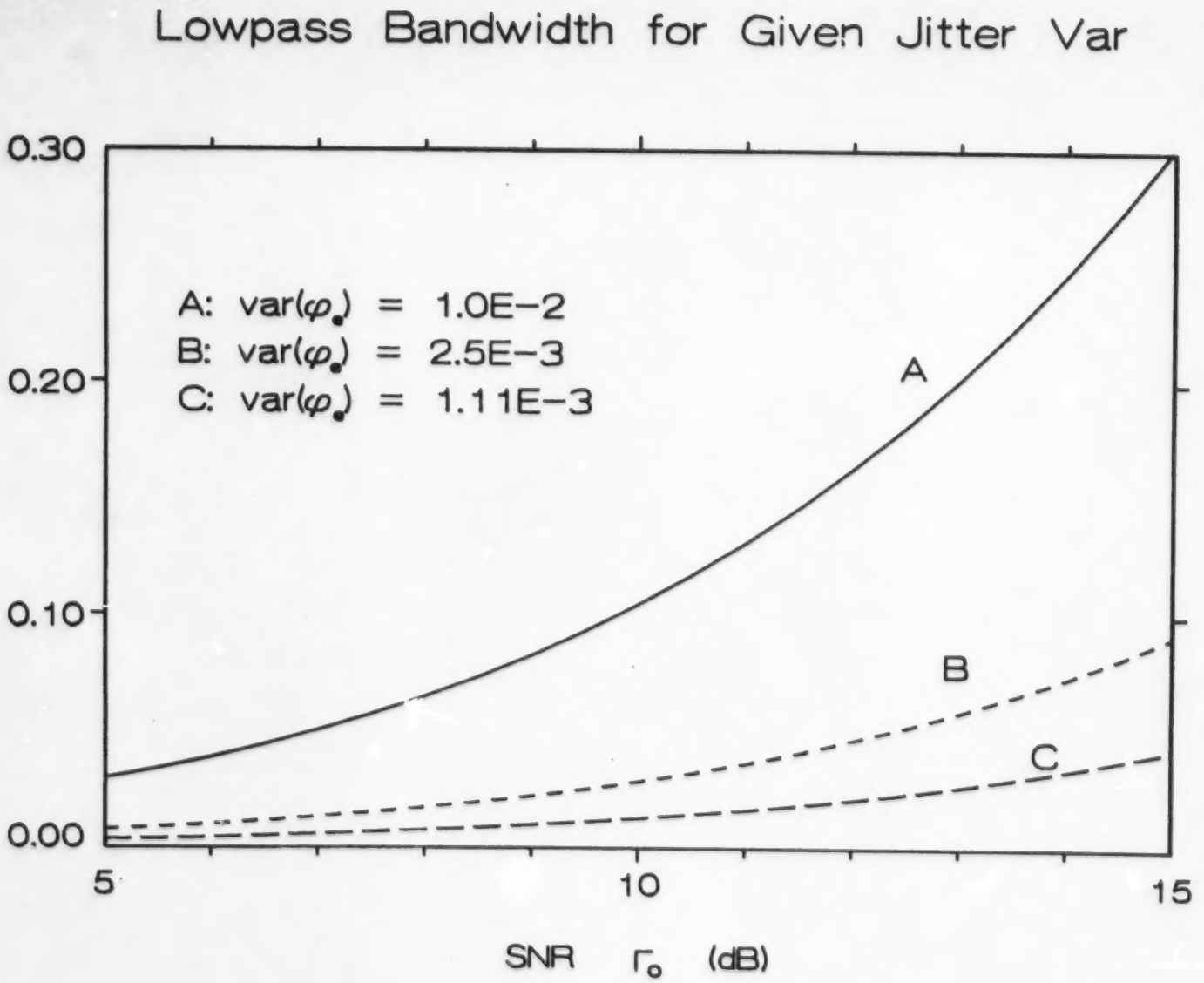

Figure 8 Lowpass Bandwidth With Fixed Jitter Variance

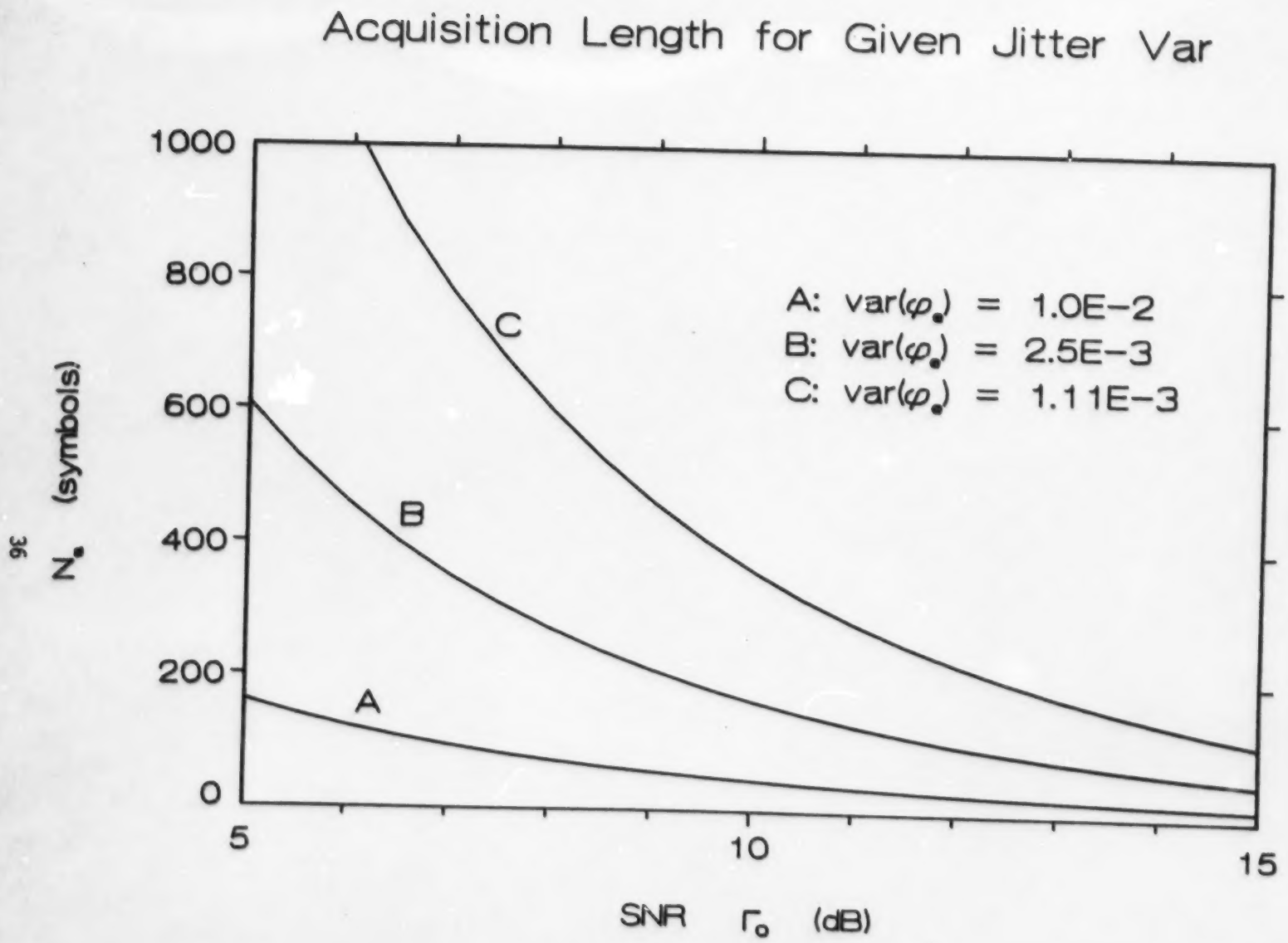

Figure 9 Acquisition Time With Fixed Jitter Variance

Centre for Systems Science

• Simon Fraser University established the **Centre for Systems Science** as a provincial centre for advanced study. The objective of CSS is twofold: coordinate and combine advanced systems research at SFU, and encourage application of research results within industry in order to further the technological development of British Columbia.

• CSS has assembled three research groups to streamline its efforts. The orientation of these groups is as follows: intelligent systems, microelectronics, and computer and communications systems. Because of shared research interests, this latter group merges with LCCR (**Laboratory for Computer and Communications Research**) for the publication of technical reports.

• CSS's three groups involve over 80 skilled faculty researchers principally from SFU's Schools of Engineering Science and Computing Science, but also draw substantially on Mathematics, Physics, Geography, Philosophy, Linguistics, Psychology, Communication, and Kinesiology.